Perilipin 3 Deficiency Stimulates Thermogenic Beige Adipocytes Through *PPARα* Activation

Yun Kyung Lee,[1] Jee Hyung Sohn,[1] Ji Seul Han,[1] Yoon Jeong Park,[1,2] Yong Geun Jeon,[1] Yul Ji,[1] Knut Tomas Dalen,[3] Carole Sztalryd,[4] Alan R. Kimmel,[5] and Jae Bum Kim[1,2]

Diabetes 2018;67:791–804 | https://doi.org/10.2337/db17-0983

Beige adipocytes can dissipate energy as heat. Elaborate communication between metabolism and gene expression is important in the regulation of beige adipocytes. Although lipid droplet (LD) binding proteins play important roles in adipose tissue biology, it remains unknown whether *perilipin 3* (*Plin3*) is involved in the regulation of beige adipocyte formation and thermogenic activities. In this study, we demonstrate that *Plin3* ablation stimulates beige adipocytes and thermogenic gene expression in inguinal white adipose tissue (iWAT). Compared with wild-type mice, *Plin3* knockout mice were cold tolerant and displayed enhanced basal and stimulated lipolysis in iWAT, inducing peroxisome proliferator–activated receptor α (*PPARα*) activation. In adipocytes, *Plin3* deficiency promoted *PPARα* target gene and uncoupling protein 1 expression and multilocular LD formation upon cold stimulus. Moreover, fibroblast growth factor 21 expression and secretion were upregulated, which was attributable to activated *PPARα* in *Plin3*-deficient adipocytes. These data suggest that *Plin3* acts as an intrinsic protective factor preventing futile beige adipocyte formation by limiting lipid metabolism and thermogenic gene expression.

Adipose tissues are actively engaged in the regulation of energy homeostasis to respond to dynamic changes in obesity and cold acclimation (1,2). In mammals, adipose tissues have been traditionally classified into white adipose tissue (WAT) and brown adipose tissue (BAT). These two types of adipose tissues differ in various aspects, including anatomical locations, cellular morphologies, and metabolic characteristics. In WAT, adipocytes usually contain a large and unilocular lipid droplet (LD) and prominently maintain energy homeostasis not only by acting as a major energy depot but also by releasing various adipokines and lipid metabolites that have numerous effects on metabolic tissues (3,4). In contrast, BAT primarily governs nonshivering thermogenesis as well as energy expenditure in response to cold (2,3,5,6). BAT has uncoupling protein 1 (UCP1)–positive brown adipocytes that are packed with small and multilocular LDs and abundant mitochondria, leading to the dissipation of chemical energy in the form of heat (1,2,5,6). Recently, a new, distinct type of thermogenic adipocytes intermingled within WAT has been identified; these adipocytes were termed "beige" or "brite" adipocytes. In rodents, beige adipocytes are found in inguinal WAT (iWAT) upon cold or β-adrenergic stimuli and share several key characteristics with brown adipocytes including multilocular LDs, high mitochondrial density, and UCP1 expression (7,8). Nevertheless, brown and beige adipocytes arise from distinct developmental lineages with different features (7,9). Recent studies have shown that beige adipocytes appear to arise from transdifferentiation of mature white adipocytes (10,11) as well as de novo differentiation from beige adipocyte precursors (12,13). Upon cold exposure, hormones such as norepinephrine rewire transcriptional execution and metabolic regulation to induce beige/brite adipocyte differentiation in iWAT (1,14,15). In contrast, classic brown adipocytes originate from muscle-like cell lineages (9,16).

In eukaryotic cells, accumulated LDs contain neutral lipids, including triacylglycerides (TAGs) and cholesteryl

[1]Department of Biological Sciences, National Creative Research Initiatives Center for Adipose Tissue Remodeling, Institute of Molecular Biology and Genetics, Seoul National University, Seoul, South Korea
[2]Department of Biophysics and Chemical Biology, Seoul National University, Seoul, South Korea
[3]Department of Nutrition, Institute of Basic Medical Sciences, University of Oslo, Oslo, Norway
[4]Department of Medicine, University of Maryland School of Medicine, Baltimore, MD
[5]Laboratory of Cellular and Developmental Biology, National Institute of Diabetes and Digestive and Kidney Diseases, National Institutes of Health, Bethesda, MD

Corresponding author: Jae Bum Kim, jaebkim@snu.ac.kr.

Received 17 August 2017 and accepted 5 February 2018.

This article contains Supplementary Data online at http://diabetes.diabetesjournals.org/lookup/suppl/doi:10.2337/db17-0983/-/DC1.

© 2018 by the American Diabetes Association. Readers may use this article as long as the work is properly cited, the use is educational and not for profit, and the work is not altered. More information is available at http://www.diabetesjournals.org/content/license.

esters, surrounded by a phospholipid monolayer. LDs are coated with LD-associated proteins such as perilipins (Plins) (17). In mammals, the Plin family is composed of five members, namely, Plin1 through 5. Among the five Plin isoforms, Plin1 has been identified as the major LD-coating protein in adipocytes (18). It has been suggested that Plins modulate intracellular lipid metabolism by regulating TAGs and cholesteryl esters within LDs in various cell types. For instance, *Plin1* knockout (KO) mice have enhanced lipolysis in WAT and are resistant to diet-induced obesity (19,20). Moreover, adipose tissue–specific overexpression of *Plin1* results in the reduction of LD size as well as WAT mass (21,22). Also, *Plin2* KO mice are protected against hepatic lipid accumulation (17), whereas hepatic overexpression of *Plin2* increases cellular TAGs and LD size, with reduced lipolysis (23). In addition, it has been reported that *Plin5* plays a role in the regulation of LD hydrolysis in oxidative tissues (24,25). Thus, it appears that Plins stabilize and remodel intracellular LDs and influence lipid mobilization and utilization to regulate energy homeostasis. Nonetheless, the functional roles of *Plin3* in adipocytes have not yet been thoroughly established.

In this study, we demonstrate that *Plin3* deficiency enhances thermogenesis and beige adipocyte differentiation in iWAT by stimulating lipolysis and thermogenic gene expression. iWAT and differentiated adipocytes were examined for lipid metabolism and beige adipocyte gene index to gain mechanistic insights. In adipocytes, *Plin3* deficiency stimulated fatty acid (FA) oxidation and the activity of peroxisome proliferator–activated receptor α (*PPARα*), one of the thermogenic transcription factors. To further investigate the roles of *Plin3* in vivo, morphological changes and gene expression profiles in adipose tissues were scrutinized in *Plin3* KO mice. In *Plin3* KO mice, the expression of fibroblast growth factor 21 (FGF21) was augmented, at least partly, through *PPARα* activation. These data suggest that *Plin3* might function as a negative regulator of thermogenesis in iWAT by limiting the availability of lipid metabolites.

RESEARCH DESIGN AND METHODS

Animals and Metabolic Experiments

Plin3 KO mice were generated with the guidelines of the Animal Care and Use Committee of the National Institutes of Health. All animal experiments were conducted in compliance with protocols approved by the Institutional Animal Care and Use Committee at the Seoul National University (SNU-130508). Mice were maintained at 22–24°C in 12-h light/dark cycles and fed ad libitum with a standard rodent chow diet. For the cold tolerance test, 8–10-week-old male mice were placed in a cold room at 4°C (Testo Inc., Sparta, NJ) for 8 h. For thermoneutral and cold-exposure experiments, 8–10-week-old male mice were placed at 30°C for 7 days and then split into two groups: one group was exposed to thermoneutral condition and the other group to cold for 6 days. At the end of experiments, serum samples were collected. Free FAs (FFAs; Roche, Indianapolis, IN) and FGF21 (Antibody and Immunoassay Services, Pokfulam, Hong Kong) were measured according to the manufacturers' protocols. Tissue samples were frozen for further analyses.

Thermal Imaging

The surface temperature of the mice was imaged using an infrared camera (CX320 Thermal Imaging Camera; COX Co., Seoul, Korea).

RNA Preparation and Reverse Transcription Quantitative PCR

RNA was extracted from cultured cells or frozen tissue samples using TRIzol (Ambion, Foster City, CA). For reverse transcription quantitative PCR (qRT-PCR), 1–3 μg total RNA was reverse-transcribed using the High-Capacity cDNA Reverse Transcription kit (Thermo Fisher Scientific, Waltham, MA). SYBR Green reactions using the SYBR Green PCR Master mix (Enzynomics, Daejeon, South Korea) were assembled along with 10 pmol/L primers according to the manufacturer's instructions. All primers used are listed with their sequences in Supplementary Table 1.

Adipocyte Differentiation and Cell Culture Experiments

Stromal vascular cells were prepared as previously reported (26) with minor modifications. Briefly, iWAT was dissected and washed with PBS, minced, and digested by collagenase I (Worthington Biochemical, Lakewood, NJ). Differentiation was initiated as described elsewhere (27). For small interfering RNA (siRNA) experiments to suppress *PPARα* or *PPARγ*, differentiated adipocytes were differentiated and transiently transfected with Lipofectamine 2000 (Invitrogen, Carlsbad, CA) according to the manufacturer's protocol. siRNA duplexes were designed and purchased from Bioneer (Daejeon, South Korea; *PPARα*, 1411367; *PPARγ*, 1411392). At 24 h posttransfection, cells were treated with isoproterenol (Sigma-Aldrich, St. Louis, MO) or an equal amount of double-distilled H_2O in serum-free DMEM. After incubation for 6–8 h, the cells were harvested for further analyses. To assess the effects of *PPARα* agonist and *PPARα* antagonist, cells pretreated with WY-14643 (Sigma-Aldrich) and GW-6471 (Sigma-Aldrich) for 48 h. Media were changed to DMEM containing 2% FA-free BSA, and cells were stimulated with 3 μmol/L isoproterenol or an equal amount of double-distilled H_2O for 6–8 h.

Lipolysis

Differentiated mature adipocytes were chased with DMEM containing 2% FA-free BSA and treated with 50 μmol/L H-89 (Sigma-Aldrich) and/or 1 μmol/L isoproterenol. The levels of glycerol released into supernatants were quantified using a commercial kit (Sigma-Aldrich). Amounts of glycerol were normalized to the total protein content of the differentiated adipocytes using a Pierce BCA protein assay reagent (Thermo Fisher Scientific).

Immunoblotting and Histological Analysis

For immunoblotting, proteins were extracted and separated by SDS-PAGE and then transferred to nitrocellulose membranes

(Bio-Rad, Hercules, CA). The membranes were probed with primary antibodies against UCP1 (Abcam, Cambridge, MA) followed by horseradish peroxidase–conjugated secondary antibody (Santa Cruz Biotechnology, Santa Cruz, CA). GAPDH was used as a loading control (Sigma-Aldrich). Band intensities were quantified using ImageJ (National Institutes of Health, Bethesda, MD). For immunohistochemistry, adipose tissues were fixed in 4% paraformaldehyde and embedded in paraffin. Adipose tissues were stained with hematoxylin and eosin (H&E) or for UCP1. According to a previous report (28), quantitation of UCP1-positive adipocytes was carried out.

Mitochondrial Activity and Mitochondrial Nuclear DNA Quantification

For JC-1 staining, isolated mitochondria were incubated with 5 μg/mL JC-1 probe (Thermo Fisher Scientific) and then visualized under a Zeiss LSM 710 microscope (Carl Zeiss, Oberkochen, Germany). Total DNA from iWAT was extracted using the DNeasy blood and tissue kit (Qiagen, Germantown, MD), and the relative levels of mitochondrial DNA and nuclear DNA were quantified using primers specific for mitochondrial *16S* rRNA and nuclear *18S* rRNA genes. qRT-PCR primers are listed in Supplementary Table 1.

Cellular Oxygen Consumption

Cellular oxygen consumption rates (OCRs) of differentiated adipocytes were analyzed by Seahorse XF^{e}24 extracellular flux analyzer (Seahorse Bioscience, North Billerica, MA) according to the manufacturer's instruction. Mitochondrial proteins were isolated by the manufacturer's protocol (Abcam). Values are normalized to average basal respiration.

Luciferase Assay

HEK293 cells were transiently transfected with various DNA plasmids (*PPARα*, *retinoid X receptor α* [*RXRα*], *β-galactosidase*, and DR-1) by the calcium-phosphate method, as described previously (29). Luciferase and β-galactosidase activities were measured according to the manufacturer's protocol (Promega, Madison, WI). Relative luciferase activity was normalized to β-galactosidase activity in each sample.

Statistical Analysis

All values in graphs are presented as the mean ± SEM. Student *t* test was used for single comparisons. The error bars (SEM) shown for all results were derived from biological, not technical, replicates. Significant differences between two groups ($^*P < 0.05$; $^{**}P < 0.01$; $^{***}P < 0.001$) were evaluated by two-tailed unpaired *t* tests as the sample groups or by two-way ANOVA when two conditions were involved (GraphPad Software, La Jolla, CA).

RESULTS

Plin3-Deficient Mice Are Cold Tolerant, With Increased Beige Adipocytes in iWAT

Unlike Plin1, Plin3 protein was ubiquitously expressed in various tissues, including WAT and BAT (Supplementary Fig. 1*A*). To further investigate the roles of *Plin3* in lipid metabolism and fat tissue biology, we generated *Plin3* KO mice with deletion of exons 3, 4, and 5 encoding the LD-binding domain of *Plin3* (Supplementary Fig. 1*B* and *C*). *Plin3* KO mice were born at Mendelian ratios and morphologically normal (Supplementary Fig. 1*D*). Even though body and various metabolic tissue weights of *Plin3* KO mice were comparable to those of wild-type (WT) mice, LD morphologies in several adipose tissues including BAT, epididymal WAT, and iWAT of *Plin3* KO mice were distinguishable from those of WT mice (Fig. 1).

Given that the formation of multilocular LDs in WAT and BAT is one of the key phenotypic changes induced by thermogenic stimulation (7,30), we raised the question whether an increase in the number of adipocytes with multilocular LDs in adipose tissues of *Plin3* KO might be associated with cold tolerance. Under thermoneutral (30°C) and cold temperature (4°C), body weight and the weights of several tissues including liver, epididymal WAT, iWAT, and BAT were not different between WT and *Plin3* KO mice (Supplementary Fig. 2*A*). Interestingly, *Plin3* KO mice were more cold tolerant than WT mice (Fig. 2*A*). Also, infrared imaging analysis revealed that cold-exposed *Plin3* KO mice generated higher body temperature (Fig. 2*B*). At thermoneutral temperature, iWAT of *Plin3* KO mice showed smaller adipocytes, with multilocular LDs, than iWAT of WT mice (Fig. 2*C*). Under cold conditions, the formation of small and multilocular LDs in iWAT was greatly increased in *Plin3* KO mice as compared with WT mice (Fig. 2*C*). At thermoneutral temperature, mRNA of *UCP1*, a surrogate thermogenic marker, was barely detectable in iWAT from WT and *Plin3* KO mice (Fig. 2*D*). On the contrary, compared with WT mice, *UCP1* mRNA expression was markedly increased in iWAT from *Plin3* KO mice upon cold stimulation. In addition, mRNA levels of other thermogenic genes including *PGC1α*, *Elovl3*, *Dio2*, and *Cidea* were greatly elevated in iWAT of *Plin3* KO mice (Fig. 2*D*). Moreover, mRNA levels of beige adipocyte–specific genes including *CD137*, *Tbx1*, *TMEM26*, and *Slc27a1* were further elevated in iWAT of *Plin3* KO mice upon cold stimulation (Supplementary Fig. 2*B*). In BAT, *Plin3* deficiency led to a reduction in LD size at thermoneutral temperature, whereas the size and shape of LDs were comparable between WT and *Plin3* KO mice under cold stimulation (Fig. 2*E*). Compared with BAT of WT mice, mRNA levels of the thermogenic genes such as *UCP1*, *PGC1α*, *Elovl3*, *Dio2*, and *Cidea* were not significantly altered in BAT of *Plin3* KO mice under both thermoneutral and cold temperatures (Fig. 2*F*). In accordance with these, *Plin3* KO mice exhibited higher body temperature and energy expenditure than WT mice in the presence of CL-316,243, β3-adrenergic receptor agonist (Supplementary Fig. 2*C* and *D*). At room temperature, mRNA levels of thermogenesis, FA oxidation, and mitochondrial-related genes were slightly but not dramatically increased in *Plin3* KO in iWAT (Supplementary Fig. 2*E*). Also, *Plin3* KO mice appeared to exhibit elevated whole-body energy metabolism parameters at room temperature (Supplementary Fig. 2*F*). Taken together, these data indicate that *Plin3*

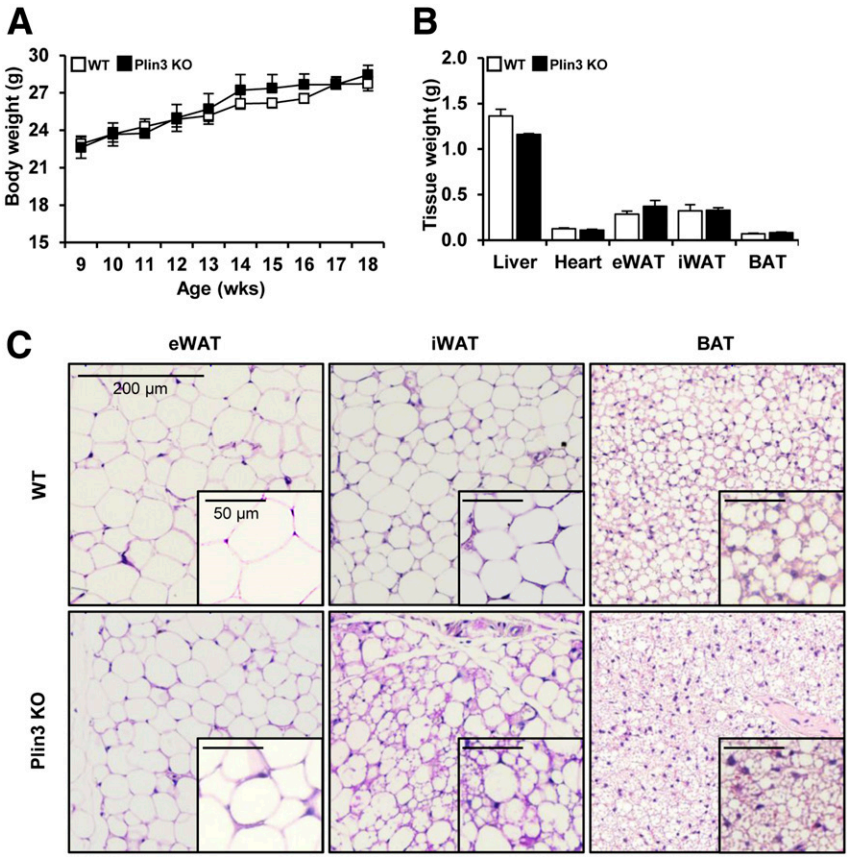

Figure 1—*Plin3* deficiency stimulates the formation of small and multilocular LDs containing adipocytes. *A*: Body weights of WT and *Plin3* KO mice at room temperature (n = 10 to 11 mice/group). *B*: Tissue weights in WT and *Plin3* KO mice at 8–10 weeks of age (n = 6 mice/group). Mice were fed a normal chow diet. *C*: Representative images of H&E staining of adipose tissues of WT and *Plin3* KO mice. Mice were fed a normal chow diet and grown at room temperature. Scale bars, 200 μm. The insets show LD morphology for each tissue at a higher magnification. Scale bars, 50 μm (n = 3 mice/group). Data represent the mean ± SEM. eWAT, epididymal WAT.

deletion would induce cold resistance and potentiates thermogenic gene expression in iWAT.

Plin3 Deficiency Activates UCP1 Expression in iWAT Upon Cold Exposure

As beige adipocytes are characterized by enhanced UCP1 expression and thus contribute to thermogenic activity (8,11), we examined the expression level of UCP1 protein in iWAT. Under thermoneutral conditions, UCP1 protein was hardly detected in iWATs from both WT and *Plin3* KO mice, whereas UCP1 protein was greatly upregulated in cold-exposed iWAT from *Plin3* KO mice (Fig. 3*A* and *B*). Even though UCP1 protein was abundantly expressed in BAT under thermoneutral and cold conditions, the extent of UCP1 protein induction in BAT was lower than that in iWAT at cold conditions. At thermoneutral temperatures, the number of UCP1-positive adipocytes in iWAT did not differ between WT and *Plin3* KO mice (Fig. 3*C* and *D*). In contrast, compared with cold-stimulated iWAT of WT mice, cold-stimulated iWAT of *Plin3* KO mice showed more UCP1-positive adipocytes (Fig. 3*C* and *D*). However, BAT from WT or *Plin3* KO mice exhibited similar abundances of UCP1-positive adipocytes at both thermoneutral and cold temperatures (Fig. 3*E* and *F*). As cold condition increased UCP1 expression in BAT from WT and *Plin3* KO to a comparable extent, it appeared that iWAT, rather than BAT, might primarily contribute to the augmented thermogenic activity in *Plin3* KO mice upon cold exposure. Collectively, these results suggest that deletion of *Plin3* could stimulate UCP1-positive beige adipocytes in iWAT in response to cold exposure.

Plin3 Deficiency Leads to an Increase in Lipolysis

Plins have been implicated in the regulation of LD either through engaging in lipid storage or utilization (19,20,24). This led us to test whether TAG hydrolysis might be involved in small and multilocular LD formation in iWAT of *Plin3* KO mice. When we analyzed the serum level of FFAs, it was not different in WT and *Plin3* KO mice at thermoneutral temperature. However, after cold exposure, serum FFAs were significantly higher in *Plin3* KO than in WT mice (Fig. 4*A*). In addition, the level of TAG in iWAT was decreased to a further extent in *Plin3* KO mice upon cold stimulation (Fig. 4*B*). Next, we examined lipolytic activities by measuring FFAs and glycerol. Although the levels of FFAs and glycerol in iWAT from WT mice were similar to

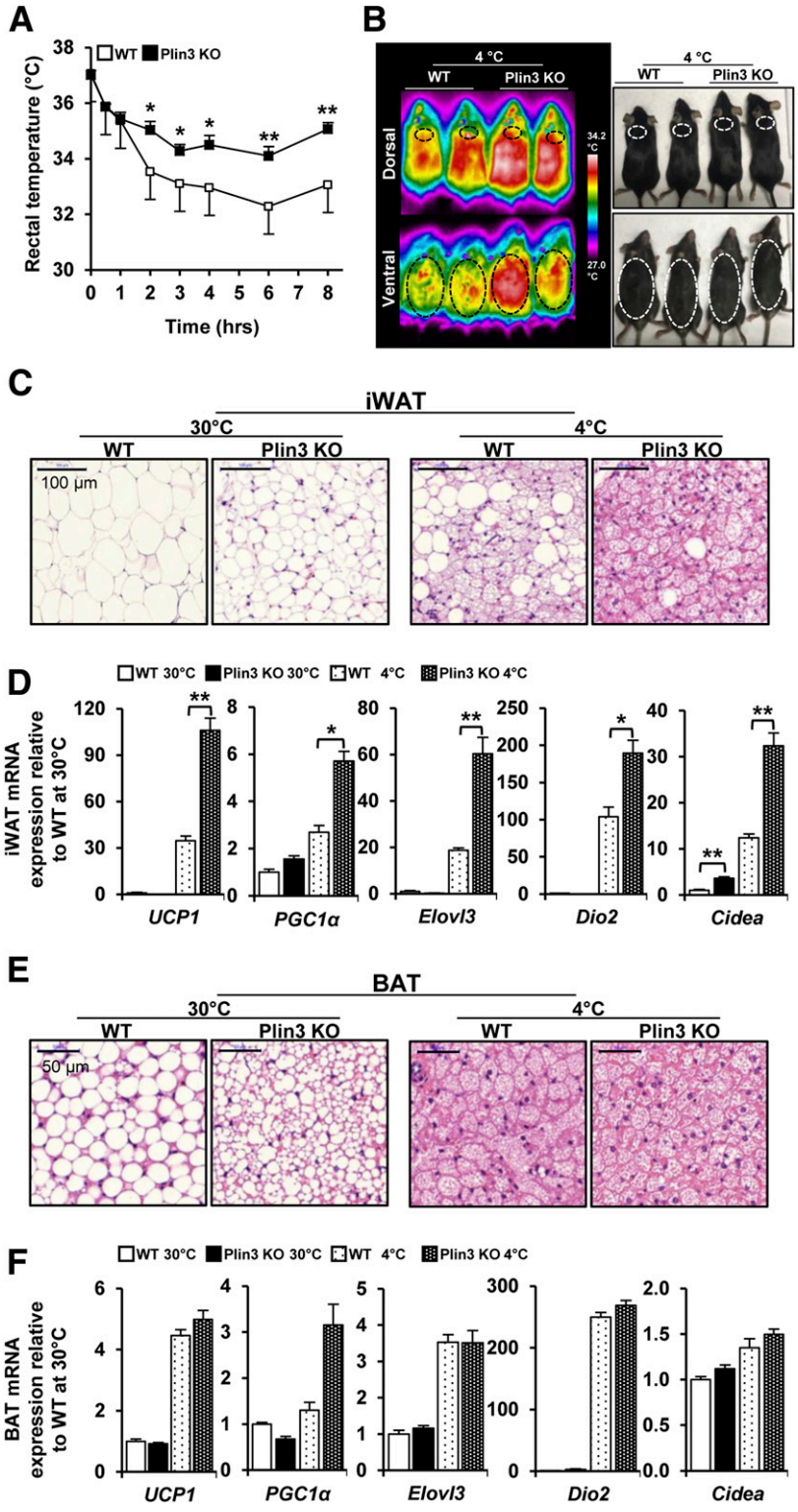

Figure 2—*Plin3* KO mice are cold tolerant and contain multilocular LDs in adipose tissues. *A*: Changes in rectal temperature during cold exposure (n = 6 mice/group, three independent experiments). *B*: Infrared (left) and photographic (right) images of surface body temperature of WT and *Plin3* KO mice after cold exposure (n = 2 mice/group). *C*: Representative images of H&E staining of iWAT at 30°C or 4°C for 6 days (n = 3 mice/group). Scale bars, 100 μm. *D*: qRT-PCR analysis for thermogenic gene expression in iWAT of WT and *Plin3* KO mice (n = 6 mice/group). Each mRNA level was normalized to *cyclophilin* mRNA, and mRNA expression levels are relative to WT at 30°C. *E*: Representative images of H&E staining of BAT at 30°C or 4°C for 6 days (n = 3 mice/group). Scale bars, 50 μm. *F*: qRT-PCR analysis for thermogenic gene expression in BAT of WT and *Plin3* KO mice (n = 6 mice/group). Each mRNA level was normalized to *cyclophilin* mRNA, and mRNA expression levels are relative to WT at 30°C. Data represent the mean ± SEM. $^*P < 0.05$; $^{**}P < 0.01$ indicate significant differences between groups as determined by either two-tailed unpaired Student t tests or two-way ANOVA versus control.

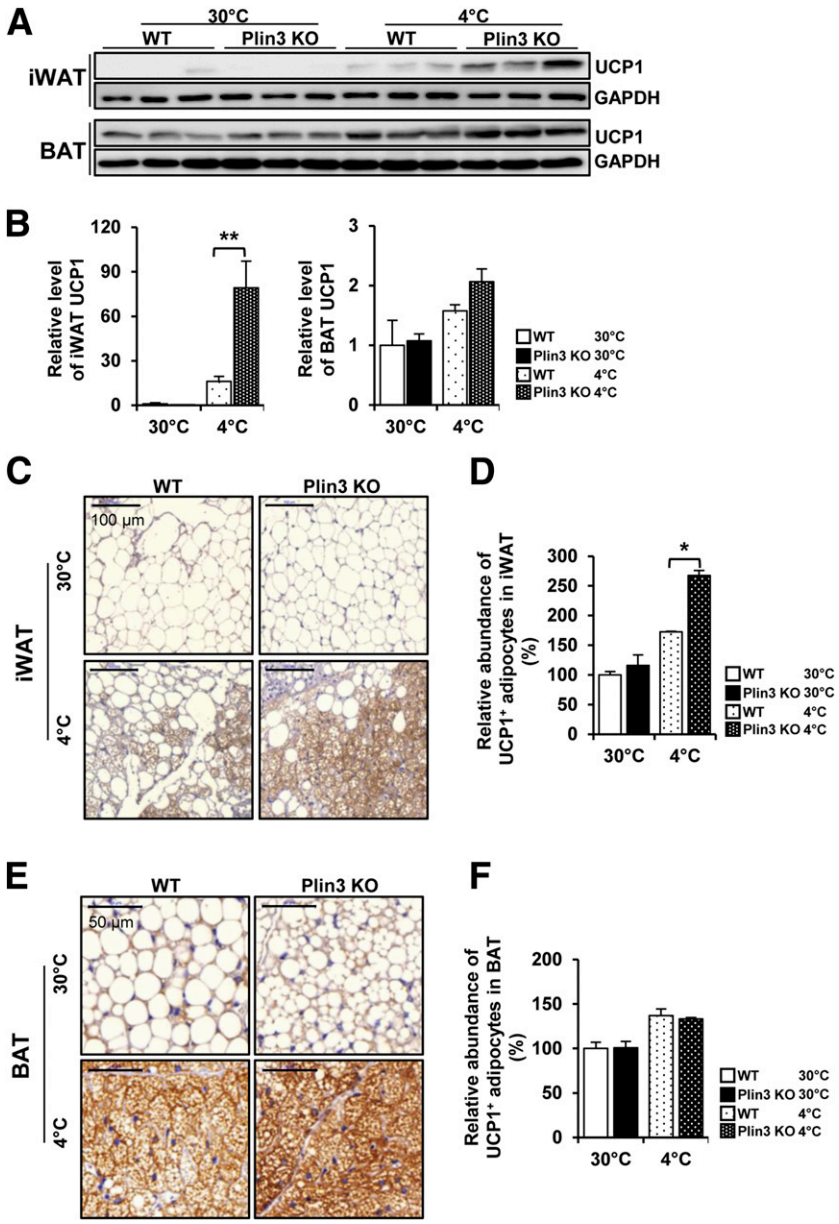

Figure 3—*Plin3* deficiency increases UCP1 expression in iWAT upon cold exposure. *A*: Immunoblots for UCP1 protein in iWAT and BAT of WT and *Plin3* KO mice exposed to 30°C or 4°C for 6 days (n = 3 mice/group). GAPDH was used as a loading control. *B*: Quantitation of UCP1 protein levels in *A* and normalized to GAPDH protein. UCP1 levels are relative to WT at 30°C. *C*: Immunohistochemical staining of UCP1 in iWAT of WT and *Plin3* KO mice exposed to 30°C or 4°C for 6 days (n = 3 mice/group). Scale bars, 100 μm. *D*: Quantitation of UCP1-positive adipocytes in *C*. UCP1 levels are relative to WT at 30°C. *E*: Immunohistochemical staining of UCP1 in BAT of WT and *Plin3* KO mice exposed to 30°C or 4°C for 6 days (n = 3 mice/group). Scale bars, 50 μm. *F*: Quantitation of UCP1-positive adipocytes in *E*. UCP1 levels are relative to WT at 30°C. Data represent the mean ± SEM. $^*P < 0.05$; $^{**}P < 0.01$ indicate significant differences between groups as determined by either two-tailed unpaired Student *t* tests or two-way ANOVA versus control.

those of *Plin3* KO mice at thermoneutral temperatures, both metabolites were further upregulated in cold-exposed iWAT of *Plin3* KO mice (Fig. 4*C*), implying that iWAT of *Plin3* KO mice appeared to be readily lipolytic in response to cold stimulation. Then, to determine whether increased lipolysis in *Plin3*-ablated iWAT might be cell autonomous, differentiated adipocytes from WT and *Plin3* KO mice were subjected to measurement of lipolytic activities. To mimic cold exposure through β-adrenergic activation, differentiated adipocytes were treated with isoproterenol, a β-adrenergic activator. As shown in Fig. 4*D*, the level of released glycerol was further elevated in isoproterenol-treated *Plin3* KO adipocytes, but not in *Plin3* KO brown adipocytes (Supplementary Fig. 3). To confirm the increased lipolytic capacity of *Plin3*-deficient adipocytes, we examined downstream signaling cascade of protein kinase A (PKA), which is the key factor to mediate lipolysis. Compared with WT adipocytes, the phosphorylation levels of PKA substrates (Ser/Thr) and

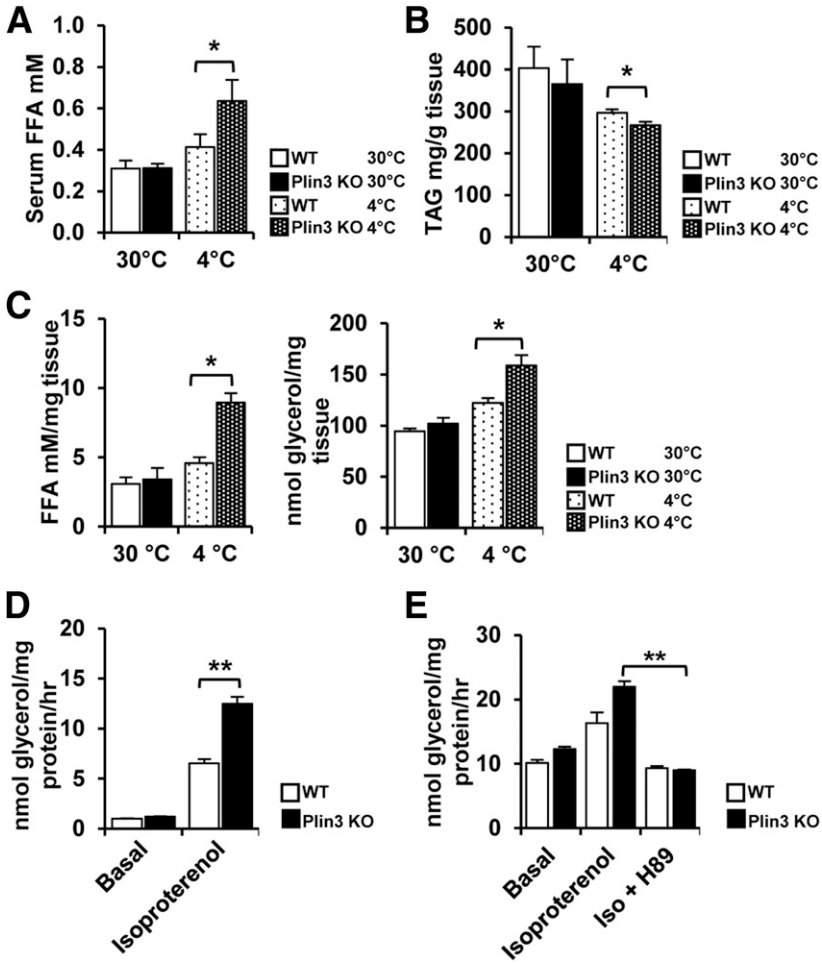

Figure 4—*Plin3* deficiency promotes lipolysis upon cold or isoproterenol stimulus. *A*: Serum FFA levels in WT and *Plin3* KO mice exposed to 30°C or 4°C (n = 3–5 mice/group). *B*: TAG levels in iWAT from WT and *Plin3* KO mice exposed to 30°C or 4°C (n = 4 to 5 mice/group). *C*: FFA and glycerol levels in iWAT from WT and *Plin3* KO mice exposed to 30°C or 4°C (n = 3–5 mice/group). *D*: Stromal vascular cells were isolated from iWAT of WT and *Plin3* KO mice and fully differentiated into adipocytes. For basal and stimulated lipolysis, differentiated adipocytes were treated with or without isoproterenol (1 μmol/L) for 3 h. The levels of glycerol were measured from conditional media. *E*: Differentiated adipocytes pretreated with or without H-89 (50 μmol/L; an inhibitor of PKA) followed by isoproterenol (Iso; 1 μmol/L) for 3 h. The levels of glycerol were measured from conditional media. Data represent the mean ± SEM. $^*P < 0.05$; $^{**}P < 0.01$ indicate significant differences between groups as determined by either two-tailed unpaired Student t tests or two-way ANOVA versus control.

hormone-sensitive lipase (Ser^{563}) were further increased in *Plin3*-deficient adipocytes upon isoproterenol (Supplementary Fig. 4*A*). In the LD fraction of *Plin3*-deficient adipocytes, the levels of ATGL and CGI58 proteins seemed to be further enhanced upon isoproterenol (Supplementary Fig. 4*B*). When PKA was inhibited by H-89, increased lipolytic activity in *Plin3* KO adipocytes was nullified (Fig. 4*E*), implying that PKA might mediate enhanced lipolysis in *Plin3*-deficient adipocytes. Therefore, these data suggest that *Plin3* deficiency would potentiate lipolysis in iWAT upon cold stimulus.

Plin3 Deficiency Promotes Mitochondrial Activity and FA Oxidation Upon Cold Stimulus

As *Plin3* KO mice showed an enhanced induction of UCP1-positive beige adipocytes with elevated lipolytic activities during cold stimuli, we asked the question whether these cold-induced beige adipocytes in *Plin3* KO mice might have altered mitochondrial activity and biogenesis. Compared with WT iWAT, *Plin3* KO iWAT showed stronger increases in mRNA levels of the mitochondrial oxidative phosphorylation genes including *ATPase*, *CytC*, and *Cox8b* upon cold stimulation (Fig. 5*A*). To confirm this, mitochondrial OCRs were determined in differentiated adipocytes from WT and *Plin3* KO mice. As shown in Fig. 5*B*, OCRs were slightly but significantly higher in *Plin3* KO adipocytes not only in the basal state but also after stimulation with isoproterenol. The maximum respiratory capacity with carbonyl cyanide-4-(trifluoromethoxy)phenylhydrazone was further elevated in *Plin3* KO adipocytes as compared with WT adipocytes. In addition, FA oxidation rate was significantly higher in cold-exposed *Plin3* KO iWAT than in WT iWAT (Fig. 5*C*). To further investigate mitochondrial respiration capacity of iWAT, OCRs were measured in isolated mitochondria

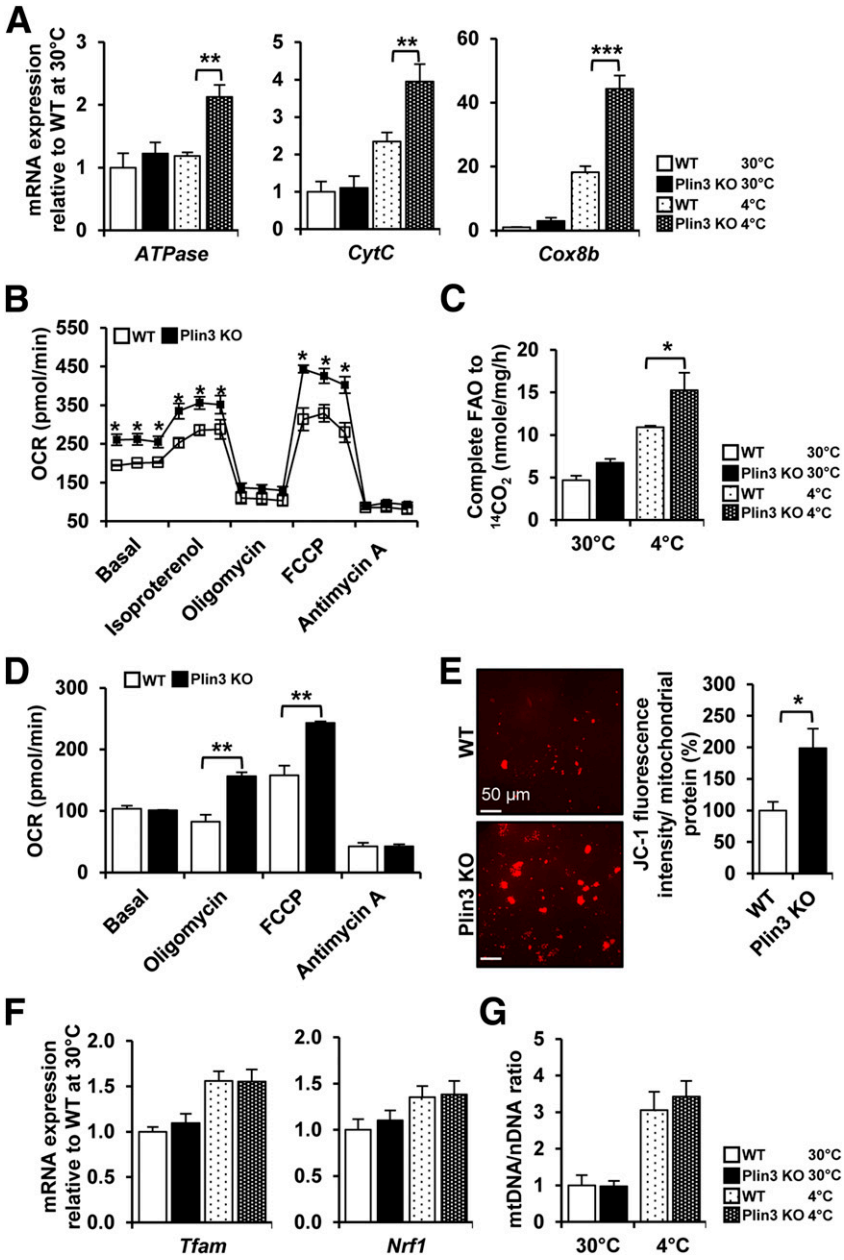

Figure 5—*Plin3* deficiency promotes mitochondrial activity and FA oxidation upon cold exposure. *A*: qRT-PCR analysis of mitochondrial gene expression in iWAT from WT and *Plin3* KO mice exposed to 30°C or 4°C (n = 3 mice/group). Each mRNA level was normalized to *cyclophilin* mRNA, and mRNA expression levels are relative to WT at 30°C. *B*: OCRs of differentiated adipocytes from iWAT of WT or *Plin3* KO mice. *C*: FA oxidation (FAO) rates in iWAT from WT or *Plin3* KO mice exposed to 30°C or 4°C (n = 4 mice/group). *D*: OCRs of isolated mitochondria from iWAT of WT or *Plin3* KO mice (n = 5 mice/group). *E*: JC-1 staining and fluorescence intensity of isolated mitochondria from iWAT of WT or *Plin3* KO mice (n = 5 mice/group). Scale bars, 50 μm. *F*: qRT-PCR analysis of mitochondrial gene expression in iWAT from WT and *Plin3* KO mice exposed to 30°C or 4°C (n = 3 mice/group). Each mRNA level was normalized to *cyclophilin* mRNA, and mRNA expression levels are relative to WT at 30°C. *G*: qRT-PCR analysis of adipose tissue mitochondrial DNA (mtDNA) contents (mtDNA/nuclear [n]DNA ratio) in iWAT from WT and *Plin3* KO mice (n = 5 mice/group). Data represent the mean ± SEM. $^*P < 0.05$; $^{**}P < 0.01$; $^{***}P < 0.001$ indicate significant differences between groups as determined by either two-tailed unpaired Student t tests or two-way ANOVA versus control. FCCP, carbonyl cyanide-4-(trifluoromethoxy)phenylhydrazone.

from WT iWAT and *Plin3* KO iWAT. As shown in Fig. 5*D*, *Plin3* deficiency showed elevated mitochondrial OCRs. Moreover, mitochondrial membrane potentials of isolated mitochondria from *Plin3* KO iWAT were higher than those from WT iWAT (Fig. 5*E*). On the contrary, both WT and *Plin3*-deficient brown adipocytes exhibited similar degrees of OCRs (Supplementary Fig. 5*A*). Given that PKA activation enhanced lipolytic capacity in *Plin3*-deficient adipocytes (Fig. 4*E*), we decided to test whether mitochondrial activity in *Plin3*-deficient adipocytes might be regulated by PKA. As shown in Supplementary Fig. 5*B*, mitochondrial activity was augmented by forskolin in *Plin3* KO adipocytes, whereas

H-89 suppressed mitochondrial membrane potentials. Nonetheless, mRNA expression of the mitochondrial biogenesis genes such as *Tfam* and *Nrf1* was not different between WT and *Plin3* KO iWATs (Fig. 5*F*), which was confirmed by mitochondrial DNA measurements (Fig. 5*G*). Together, these results propose that *Plin3* deficiency would promote mitochondrial activity and FA oxidation in cold-exposed iWAT.

PPARα Stimulates Thermogenic Beige Adipocyte Formation in *Plin3* KO Mice

To understand the molecular mechanisms underlying the promotion of beige adipocyte formation and thermogenic activation in *Plin3* KO mice, we profiled gene expression, particularly, of genes associated with lipid metabolism. Transcript levels of *PPARα* and its target genes were higher in *Plin3* KO iWAT than in WT iWAT, which was further boosted upon cold exposure (Fig. 6*A*). Then, to test whether *PPARα* would be indeed involved in the regulation of thermogenic gene expression in *Plin3* KO iWAT, differentiated adipocytes were treated with or without isoproterenol in the absence or presence of *PPARα* siRNA. Similar to the data for iWAT, adipocytes from *Plin3* KO mice expressed higher mRNA levels of *PPARα* and its target genes (Fig. 6*B*). Moreover, mRNA levels of the thermogenic genes including *UCP1*, *Elovl3*, and *Dio2* were further elevated in isoproterenol-treated *Plin3* KO adipocytes. In both WT and *Plin3* KO adipocytes, mRNA levels of thermogenic genes and *PPARα* target genes were potently attenuated by *PPARα* suppression via siRNA. To confirm the above findings, we examined the effects of activated *PPARα* with WY-14643, a synthetic agonist of *PPARα*, on the expression of thermogenic and *PPARα* target genes. Activation of *PPARα* with WY-14643 augmented the expression of thermogenic genes and *PPARα* target genes, which were more strongly elevated in *Plin3* KO adipocytes (Fig. 6*C*). Then, to evaluate the role of *PPARα* activation in *Plin3* KO adipocytes, GW-6471, a synthetic antagonist of *PPARα*, was tested in differentiated adipocytes. Similar to the results obtained with *PPARα* siRNA, inactivation of *PPARα* with GW-6471 suppressed the mRNA levels of thermogenic genes and *PPARα* target genes (Fig. 6*C*). These results indicate that *PPARα* activation would play crucial roles in upregulating thermogenic gene expression in *Plin3*-deficient adipocytes. To further investigate whether elevated *PPARα* activity in *Plin3*-deficient adipocytes might be regulated by PKA, we examined mRNA levels of *PPARα* target genes with or without forskolin and/or H-89. As shown in Supplementary Fig. 6, the mRNA levels of *PPARα* target genes were elevated by forskolin, whereas such effects were abolished by H-89, indicating that increased *PPARα* activity in *Plin3* KO adipocytes might potentiate thermogenic programing upon PKA activation. Next, to examine the possibility whether beige adipocyte formation in *Plin3* KO mice might be due to *Plin3*-deficient adipocytes in a cell-autonomous manner, we tested the effects of suppression and overexpression of *Plin3* in differentiated adipocytes. When *Plin3* was suppressed via siRNA in adipocytes, their phenotypes and gene expression pattern were similar to *Plin3* KO adipocytes (Supplementary Fig. 7). On the contrary, ectopic expression of *Plin3* would reverse overall phenotypes of *Plin3*-deficient adipocytes (Supplementary Fig. 8). These results imply that beige adipocyte formation in *Plin3* KO mice might be primarily due to *Plin3* deficiency in adipocytes.

To understand potential mechanism(s) how *PPARα* activity might be upregulated in *Plin3*-deficient adipocytes, we performed luciferase reporter assays (31,32). As shown in Fig. 6*D*, conditioned media from *Plin3*-deficient adipocytes promoted the transcriptional activity of *PPARα* with or without isoproterenol, implying that transcriptional activity of *PPARα* might be stimulated by secretory factor(s) from *Plin3* KO adipocytes. Moreover, ectopic expression of *Plin3* in *Plin3* KO adipocytes did not alter mRNA levels of *PPARα* (Supplementary Fig. 8*C*), implying that *Plin3* might not directly regulate *PPARα* expression in adipocytes. Taken together, these data propose that *Plin3*-deficient adipocytes might release unknown metabolite(s) that could stimulate *PPARα* activity.

In contrast, mRNA levels of several adipogenic and lipogenic genes under control of *PPARγ* were not different between WT and *Plin3* KO, regardless of temperature (Supplementary Fig. 9*A*–*C*). Furthermore, although the expression of these genes was equally sensitive to *PPARγ* suppression through siRNA in both WT and *Plin3* KO adipocytes in the thermogenic genes (e.g., *UCP1*, *Elovl3*, and *Dio2*), *Plin3* KO adipocytes exhibited more responsive to β-adrenergic stimulation than in WT adipocytes upon *PPARγ* suppression (Supplementary Fig. 9*D*). Collectively, these results propose that *PPARα* activation would play an important role in promoting thermogenic gene expression in *Plin3* KO adipocytes.

Plin3 Deficiency Results in Elevated FGF21 Expression

As FGF21 contributes to stimulation of beige adipocyte differentiation (33,34), we decided to test whether FGF21 might be associated with increased beige adipocytes in *Plin3* KO mice. Upon cold exposure, the level of *FGF21* mRNA was more highly elevated in iWAT of *Plin3* KO mice than in that of WT mice (Fig. 7*A*). Compared with WT adipocytes, the levels of *FGF21* mRNA and secreted FGF21 protein were enhanced in *Plin3* KO adipocytes under basal and stimulated states (Fig. 7*B*). In *Plin3*-deficient adipocytes, forskolin-induced *FGF21* expression was suppressed by H-89 (Fig. 7*C*). Next, to test whether elevated *FGF21* expression in *Plin3* KO adipocytes might be linked to *PPARα* activation, the level of *FGF21* mRNA was examined in adipocytes with or without *PPARα* suppression. Although the levels of *FGF21* mRNA were higher in *Plin3* KO than in WT adipocytes with or without isoproterenol, these were nullified by *PPARα* suppression via siRNA (Fig. 7*D*). To investigate whether *PPARα* activation was directly involved in *FGF21* expression, the effects of WY-14643 and GW-6471 on *FGF21* expression were examined. In *Plin3* KO adipocytes, *FGF21* mRNA expression was promoted by WY-14643,

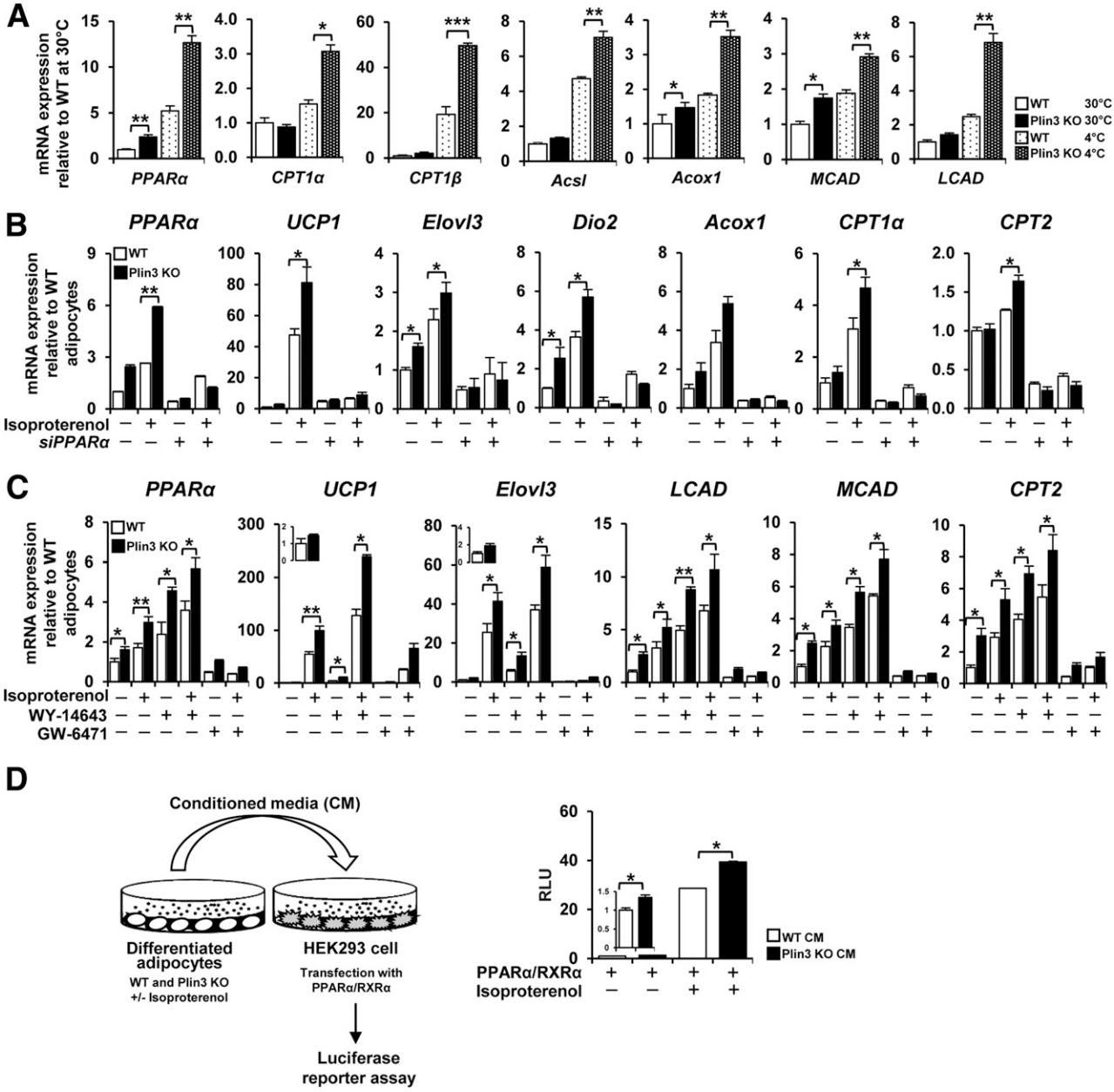

Figure 6—*PPARα* plays a crucial role to stimulate thermogenic beige adipocytes in *Plin3*-deficient iWAT. *A*: qRT-PCR analysis of FA oxidation gene expression in iWAT from WT and *Plin3* KO mice exposed to 30°C or 4°C (n = 3 mice/group). Each mRNA level was normalized to *cyclophilin* mRNA, and mRNA expression levels are relative to WT controls. *B*: qRT-PCR analysis of *PPARα* and thermogenic marker genes in differentiated adipocytes with or without *PPARα* siRNA (*siPPARα*). Differentiated adipocytes were treated with or without isoproterenol (3 μmol/L) for 8 h. Each mRNA level was normalized to *cyclophilin* mRNA, and mRNA expression levels are relative to untreated WT controls. *C*: *PPARα* and thermogenic gene expression by qRT-PCR analysis in differentiated adipocytes. Differentiated adipocytes were treated with *PPARα* agonist (WY-14643, 20 μmol/L) or *PPARα* antagonist (GW-6471, 10 μmol/L) for 48 h followed by 8-h incubation in the presence or absence of isoproterenol (3 μmol/L). *D*: *PPARα* activity by luciferase reporter assay with conditioned media (CM) from WT and *Plin3* KO adipocytes by 6-h incubation in the absence or presence of isoproterenol (3 μmol/L). Relative luciferase activity was normalized to *β-galactosidase* activity in each sample. Data represent the mean ± SEM. $^*P < 0.05$; $^{**}P < 0.01$; $^{***}P < 0.001$ indicate significant differences between groups as determined by either two-tailed unpaired Student *t* tests or two-way ANOVA versus control. RLU, relative luminescence units.

whereas it was abolished by GW-6471 (Fig. 7*E*). Together, it is likely that *PPARα* would be one of the key factors to upregulate *FGF21* expression in *Plin3* KO adipocytes, which would, at least partly, contribute to induce beige adipocyte differentiation.

In order to investigate whether *PPARα* activity would indeed be crucial in *Plin3*-deficient adipocytes, the effects of GW-6471 on thermogenic activity and *FGF21* expression were examined. In *Plin3*-deficient adipocytes, *PPARα* antagonist GW-6471 downregulated OCRs (Supplementary Fig.

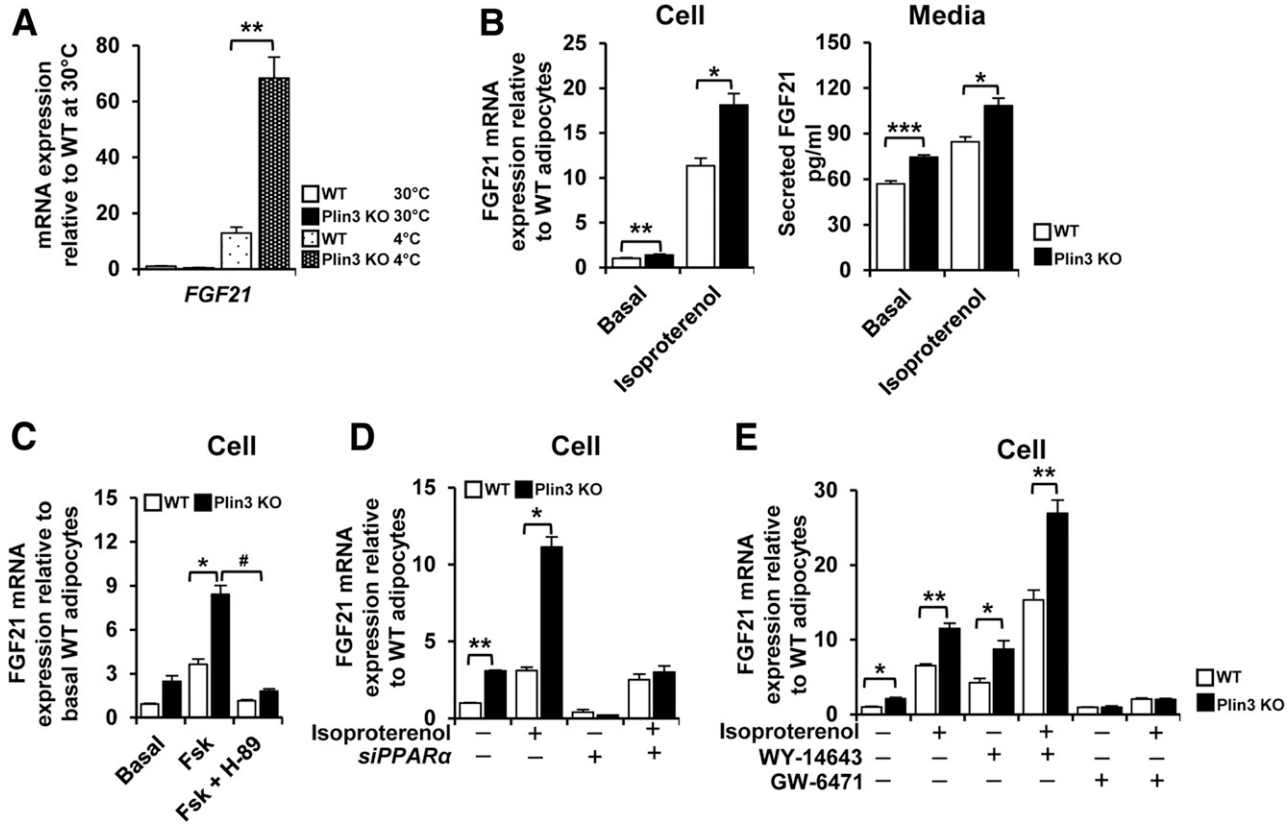

Figure 7—*Plin3* deficiency upregulates FGF21 through *PPARα* activation. *A*: qRT-PCR analysis of *FGF21* gene expression in iWAT from WT and *Plin3* KO mice exposed to 30°C or 4°C (n = 3 mice/group). *FGF21* mRNA level was normalized to *cyclophilin* mRNA, and mRNA expression levels are relative to untreated WT controls. *B*: Differentiated adipocytes from WT and *Plin3* KO mice were treated with or without isoproterenol (1 μmol/L) for 3 h. *FGF21* mRNA and secreted FGF21 proteins were determined. *FGF21* mRNA level was normalized to *cyclophilin* mRNA, and *FGF21* expression levels are relative to untreated WT controls. *C*: Differentiated adipocytes pretreated with or without H-89 (50 μmol/L) followed by forskolin (Fsk; 10 μmol/L; an activator of adenylyl cyclase) for 3 h. *FGF21* mRNA level was normalized to *cyclophilin* mRNA, and mRNA expression levels are relative to untreated WT controls. *D*: qRT-PCR analysis of *FGF21* mRNA in differentiated adipocytes with or without *PPARα* siRNA (*siPPARα*) in the presence or absence of isoproterenol (3 μmol/L) for 8 h. *E*: qRT-PCR analysis of *FGF21* mRNA in differentiated adipocytes treated with or without *PPARα* agonist (WY-14643, 20 μmol/L) or *PPARα* antagonist (GW-6471, 10 μmol/L) for 48 h followed by 8-h incubation in the presence or absence of isoproterenol (3 μmol/L). Each mRNA level was normalized to *cyclophilin* mRNA, and mRNA expression levels are relative to untreated WT controls. Data represent the mean ± SEM. *$P < 0.05$; **$P < 0.01$; ***$P < 0.001$ indicate significant differences between groups as determined by either two-tailed unpaired Student *t* tests or two-way ANOVA versus control; #$P < 0.05$ indicates significant differences between *Plin3* KO + Fsk vs. *Plin3* KO with Fsk + H-89, as determined by two-tailed unpaired Student *t* tests.

10*A*). Moreover, GW-6471 reduced rectal temperature in *Plin3* KO mice (Supplementary Fig. 10*B*). In accordance with these, mRNA levels of *PPARα* and its target genes including *Acox1*, *Acsl*, *UCP1*, and *FGF21* were abolished by GW-6471 in *Plin3* KO iWAT (Supplementary Fig. 10*C*). These results imply that *PPARα* activation would be important for thermogenic capacity of *Plin3* KO mice.

DISCUSSION

Recent studies have focused on the regulation of nonshivering thermogenesis in BAT and iWAT. However, it is largely unknown whether LD-associated proteins such as *Plin3* might contribute to modulating thermogenic beige adipocytes. In this study, we showed that *Plin3* deficiency promoted beige adipocyte formation through *PPARα* activation. *Plin3* KO mice exhibited small and multilocular LDs in iWAT and BAT, accompanied with cold tolerance. In *Plin3* KO iWAT, LD remodeling appeared to be associated with augmented thermogenic activities such as upregulated UCP1 expression and enhanced lipolysis and mitochondrial activity. Interestingly, *Plin3* KO adipocytes showed enhanced *PPARα* activation, leading to thermogenic gene expression. Therefore, these findings uncover a novel role of *Plin3* as a protective factor inhibiting unnecessary beige adipocyte formation in iWAT.

LDs are involved in lipid metabolism by storing and releasing lipid metabolites (17). Accumulating evidence suggests that *Plin*-mediated lipid metabolism might influence whole-body metabolism. For instance, it has been reported that *Plin3* is involved in obesity-induced dysregulation of lipid metabolism and insulin sensitivity in liver and skeletal muscle, respectively (35,36). In WAT, *Plin1* overexpression promotes beige adipocyte-like phenotypes through suppressing lipogenesis and *FSP27* expression (21). High-fat

diet (HFD)–fed *Plin2* KO mice showed suppression of hepatic steatosis and increased small LD-containing adipocytes, accompanied with increased *UCP1* expression in iWAT (37). To date, it has not been investigated whether *Plin3* might be involved in beige adipocyte formation as well as lipid metabolism in adipose tissue. We provided several lines of evidence that deletion of *Plin3* promoted beige adipocytes in iWAT upon cold stimuli. Firstly, *Plin3* KO mice harbored more small and multilocular LDs in iWAT at cold temperature. Secondly, mRNA levels of thermogenic genes were elevated in iWAT of *Plin3* KO mice upon cold stimuli. Moreover, *Plin3* KO mice were cold tolerant during cold exposure, implying that *Plin3* deficiency potentiated multilocular LD formation with execution of thermogenic gene reprograming to maintain body temperature under cold. Lastly, cold-stimulated UCP1 expression was elevated to a higher level in iWAT of *Plin3* KO mice than in that of WT mice. As the proportion of iWAT is greater than that of BAT in the whole body, it is plausible to speculate that iWAT of *Plin3* KO mice might primarily contribute to cold tolerance by enhancing beige adipocytes.

It has been reported that stimulation by β3-adrenergic receptor agonists or low-temperature exposure promotes lipolysis and oxidative metabolism in adipose tissue and thereby boosts thermoregulatory responses (38,39). During lipolysis, FAs are released from hydrolysis of TAG and serve as both activators and metabolic substrates for thermogenic fuels (1). Although *ATGL* KO mice and adipose-specific *CPT2* KO mice are defective for induced thermogenic activity (40,41), it remains largely unknown whether lipolysis in WAT is indeed crucial for beige adipocytes and thermogenesis for cold adaptation. In this study, we demonstrated that lipolysis and mitochondrial FA oxidation were elevated in iWAT of *Plin3* KO mice upon cold exposure, potentially, resulting in elevated thermogenic responses. Compared with WT mice, *Plin3* KO mice displayed elevated serum FFAs and reduced TAG amounts in iWAT after cold stimuli. In addition, the levels of released FFAs and glycerol were increased in iWAT of *Plin3* KO mice upon cold stimuli. Isoproterenol, as a β-adrenergic activator, mimics the changes induced by cold stimulation. Indeed, isoproterenol increased the level of released glycerol in *Plin3*-deficient adipocytes, concomitantly with elevated small and multilocular LDs. In *Plin3* KO mice, there are at least two possible pathways to promote thermogenesis in beige adipocytes upon cold: *1*) lipid metabolites might activate *PPARα* and *2*) increased FAs might augment mitochondrial activity.

Compared with other nuclear hormone receptors, *PPARs* have relatively large ligand-binding domains (42,43). Although endogenous ligands of *PPARs* have not been clearly elucidated, it has been reported that long-chain FAs are able to activate *PPARs* including *PPARα* by binding to their

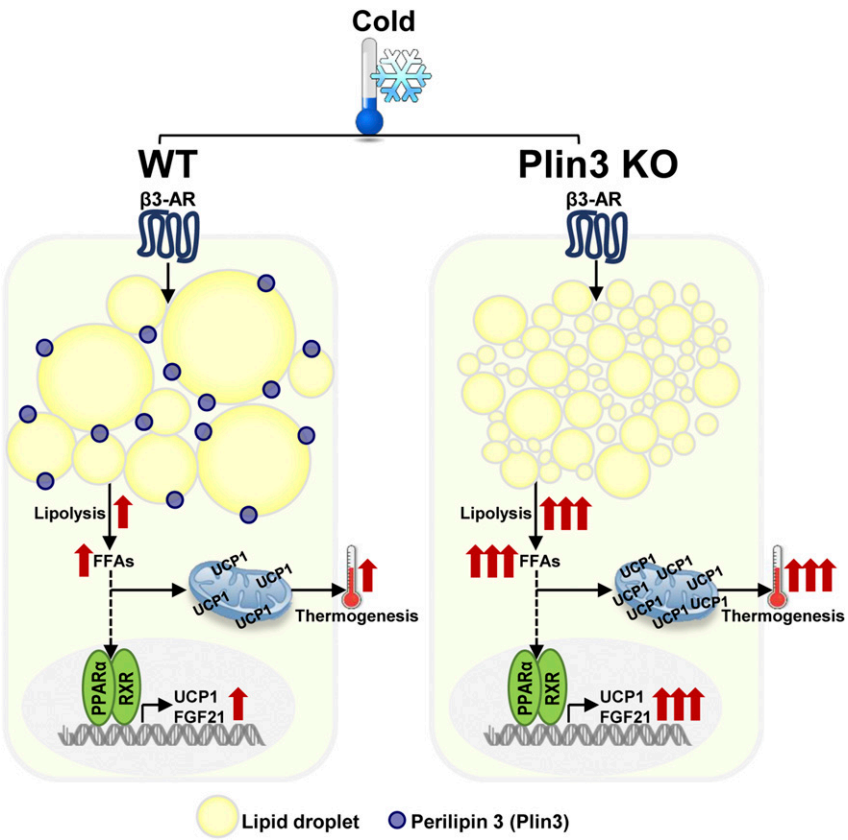

Figure 8—Schematic proposed model. In *Plin3* KO iWAT upon cold stimulation, LDs are remodeled to small and multilocular LDs that promote lipolysis and FA oxidation, leading to *PPARα* activation, to induce thermogenesis.

ligand-binding domains (44). Various lipid metabolites are able to promote thermogenic programing in adipocytes (45,46). For example, activated *PPARs* upregulate expression of *UCP1* and FA oxidation genes that are required for thermogenic activation (47,48). Moreover, it has been shown that activated *PPARα* potentiates beige adipocytes (44,49). In this study, we demonstrated that mRNA levels of *PPARα* and its target genes in iWAT of *Plin3* KO mice were promoted under cold conditions. In this regard, our following data suggested that activated *PPARα* plays a key role in potentiating beige adipocytes in *Plin3* KO mice upon cold stimulation. Firstly, suppression of *PPARα* expression downregulated expression of thermogenic genes and *PPARα* target genes in *Plin3*-deficient adipocytes. Secondly, *PPARα* agonists stimulated the expression of thermogenic genes as well as *PPARα* target genes, whereas *PPARα* antagonist abolished these responses in *Plin3*-deficient adipocytes. Lastly, in *Plin3* KO adipocytes, the level of *FGF21* expression was upregulated by activated *PPARα*, whereas inhibition of *PPARα* with either siRNA or GW-6471 nullified *FGF21* expression in *Plin3* KO adipocytes. Although *PPARγ* is a master adipogenic transcription factor and plays a crucial role in inducing beige adipocytes (50,51), it is likely that *PPARγ* is not involved in the regulation of thermogenesis or beige adipocyte differentiation in iWAT of *Plin3* KO mice. Together, these data propose that *Plin3* deletion could augment thermogenic reprograming in iWAT through *PPARα* activation.

As lipolytic products, increased FAs released from iWAT contribute to the enhancement of mitochondrial activity and UCP1 activity for thermogenic regulation. In addition, it has been reported that FAs promptly stimulate mitochondrial UCP1 activation and provide fuel for heat generation rather than ATP production (46,52). Given that iWAT of *Plin3* KO mice showed increased lipolysis, it seems that elevated lipid metabolites in iWAT of *Plin3* KO might induce UCP1-dependent thermogenesis, accompanied by enhanced mitochondrial activity and FA oxidation. In accordance with this, we observed that *Plin3* KO adipocytes exhibited increased mitochondrial activity and gene expression. We also observed that iWAT of cold-exposed *Plin3* KO mice boosted lipolysis, mitochondrial activity, and FA oxidation without altering mitochondrial biogenesis. These data imply that *Plin3* deficiency could contribute to nonshivering thermogenesis, at least partly, by upregulating mitochondrial activity and FA oxidation in iWAT. Although WAT has less oxidative capacity and lower ability to oxidize FA than BAT, rodent WAT is capable to stimulate FA oxidation in response to adrenergic activation (53). Collectively, it is likely that *Plin3*-deficient iWAT could enhance mitochondrial respiration and FA oxidation upon adrenergic activation or cold stimulus, leading to further thermogenic activities through activated *PPARα*. Compared with HFD-fed WT mice, HFD-fed *Plin3* KO mice exhibited improved metabolic phenotypes assessed by glucose tolerance test, insulin tolerance test, and lipolytic activity (Supplementary Fig. 11). Although it remains unclear how *Plin3* ablation could affect metabolic phenotypes in obesity, pathophysiological roles of *Plin3* need to be further investigated.

In summary, we demonstrate that *Plin3* deficiency in iWAT could increase lipolysis, which would activate *PPARα* to stimulate thermogenic reprograming in beige adipocytes under cold conditions (Fig. 8). Therefore, our data suggest that *Plin3* in adipose tissue might act as a barrier protein to reserve LD as an energy reservoir, which might prevent unnecessary energy burning for beige adipocyte induction.

Acknowledgments. The authors thank the members of the Laboratory of Adipocyte and Metabolism Research for helpful discussion.

Funding. This work was supported by grants from the National Creative Research Initiative Program (2011-0018312) funded by the Ministry of Education, Science and Technology. This work was also partly supported by Korea Mouse Phenotyping Project (2013M3A9D5072550) of the Ministry of Science and ICT through the National Research Foundation. This work was also supported by the Intramural Research Program of the National Institute of Diabetes and Digestive and Kidney Diseases, National Institutes of Health.

Duality of Interest. No potential conflicts of interest relevant to this article were reported.

Author Contributions. Y.K.L. designed and conducted the study, performed experiments, and wrote the manuscript. J.H.S., J.S.H., Y.G.J., and Y.J. contributed to performing animal experiments and discussed the data. Y.J.P. discussed the data and contributed to writing the manuscript. K.T.D. and C.S. contributed to the design and generation of the *perilipin 3* KO animals and discussion. A.R.K. participated in the design, generation, and propagation of the *perilipin 3* KO animals and in the editing and discussion of the manuscript. J.B.K. supervised the whole project, discussed the data, and edited the manuscript. J.B.K. is the guarantor of this work and, as such, had full access to all of the data in this study and takes responsibility for the integrity of the data and the accuracy of the data analysis.

References

1. Cannon B, Nedergaard J. Brown adipose tissue: function and physiological significance. Physiol Rev 2004;84:277–359

2. Cannon B, Nedergaard J. Nonshivering thermogenesis and its adequate measurement in metabolic studies. J Exp Biol 2011;214:242–253

3. Harms M, Seale P. Brown and beige fat: development, function and therapeutic potential. Nat Med 2013;19:1252–1263

4. Rosen ED, Spiegelman BM. Adipocytes as regulators of energy balance and glucose homeostasis. Nature 2006;444:847–853

5. Cypess AM, Chen YC, Sze C, et al. Cold but not sympathomimetics activates human brown adipose tissue in vivo. Proc Natl Acad Sci U S A 2012;109:10001–10005

6. Cypess AM, Kahn CR. Brown fat as a therapy for obesity and diabetes. Curr Opin Endocrinol Diabetes Obes 2010;17:143–149

7. Wu J, Boström P, Sparks LM, et al. Beige adipocytes are a distinct type of thermogenic fat cell in mouse and human. Cell 2012;150:366–376

8. Sidossis LS, Porter C, Saraf MK, et al. Browning of subcutaneous white adipose tissue in humans after severe adrenergic stress. Cell Metab 2015;22:219–227

9. Seale P, Bjork B, Yang W, et al. PRDM16 controls a brown fat/skeletal muscle switch. Nature 2008;454:961–967

10. Barbatelli G, Murano I, Madsen L, et al. The emergence of cold-induced brown adipocytes in mouse white fat depots is determined predominantly by white to brown adipocyte transdifferentiation. Am J Physiol Endocrinol Metab 2010;298:E1244–E1253

11. Himms-Hagen J, Melnyk A, Zingaretti MC, Ceresi E, Barbatelli G, Cinti S. Multilocular fat cells in WAT of CL-316243-treated rats derive directly from white adipocytes. Am J Physiol Cell Physiol 2000;279:C670–C681

12. Wang QA, Tao C, Gupta RK, Scherer PE. Tracking adipogenesis during white adipose tissue development, expansion and regeneration. Nat Med 2013;19:1338–1344

13. Wang QA, Scherer PE. The AdipoChaser mouse: a model tracking adipogenesis in vivo. Adipocyte 2014;3:146–150
14. Cao W, Medvedev AV, Daniel KW, Collins S. beta-Adrenergic activation of p38 MAP kinase in adipocytes: cAMP induction of the uncoupling protein 1 (UCP1) gene requires p38 MAP kinase. J Biol Chem 2001;276:27077–27082
15. Wang GX, Zhao XY, Lin JD. The brown fat secretome: metabolic functions beyond thermogenesis. Trends Endocrinol Metab 2015;26:231–237
16. Wang W, Seale P. Control of brown and beige fat development. Nat Rev Mol Cell Biol 2016;17:691–702
17. Kimmel AR, Sztalryd C. The perilipins: major cytosolic lipid droplet-associated proteins and their roles in cellular lipid storage, mobilization, and systemic homeostasis. Annu Rev Nutr 2016;36:471–509
18. Greenberg AS, Egan JJ, Wek SA, Garty NB, Blanchette-Mackie EJ, Londos C. Perilipin, a major hormonally regulated adipocyte-specific phosphoprotein associated with the periphery of lipid storage droplets. J Biol Chem 1991;266:11341–11346
19. Martinez-Botas J, Anderson JB, Tessier D, et al. Absence of perilipin results in leanness and reverses obesity in Lepr(db/db) mice. Nat Genet 2000;26:474–479
20. Tansey JT, Sztalryd C, Gruia-Gray J, et al. Perilipin ablation results in a lean mouse with aberrant adipocyte lipolysis, enhanced leptin production, and resistance to diet-induced obesity. Proc Natl Acad Sci U S A 2001;98:6494–6499
21. Sawada T, Miyoshi H, Shimada K, et al. Perilipin overexpression in white adipose tissue induces a brown fat-like phenotype. PLoS One 2010;5:e14006
22. Miyoshi H, Souza SC, Endo M, et al. Perilipin overexpression in mice protects against diet-induced obesity. J Lipid Res 2010;51:975–982
23. Imamura M, Inoguchi T, Ikuyama S, et al. ADRP stimulates lipid accumulation and lipid droplet formation in murine fibroblasts. Am J Physiol Endocrinol Metab 2002;283:E775–E783
24. Kuramoto K, Okamura T, Yamaguchi T, et al. Perilipin 5, a lipid droplet-binding protein, protects heart from oxidative burden by sequestering fatty acid from excessive oxidation. J Biol Chem 2012;287:23852–23863
25. Wang H, Sreenivasan U, Hu H, et al. Perilipin 5, a lipid droplet-associated protein, provides physical and metabolic linkage to mitochondria [published correction appears in J Lipid Res. 2013;54:3539]. J Lipid Res 2011;52:2159–2168
26. Huh JY, Kim JI, Park YJ, et al. A novel function of adipocytes in lipid antigen presentation to iNKT cells. Mol Cell Biol 2013;33:328–339
27. Ohno H, Shinoda K, Ohyama K, Sharp LZ, Kajimura S. EHMT1 controls brown adipose cell fate and thermogenesis through the PRDM16 complex. Nature 2013;504:163–167
28. Wei H, Chiba S, Moriwaki C, et al. A clinical approach to brown adipose tissue in the para-aortic area of the human thorax. PLoS One 2015;10:e0122594
29. Forman BM, Tontonoz P, Chen J, Brun RP, Spiegelman BM, Evans RM. 15-Deoxy-delta 12, 14-prostaglandin J2 is a ligand for the adipocyte determination factor PPAR gamma. Cell 1995;83:803–812
30. Okamatsu-Ogura Y, Fukano K, Tsubota A, et al. Thermogenic ability of uncoupling protein 1 in beige adipocytes in mice. PLoS One 2013;8:e84229
31. Pineda Torra I, Jamshidi Y, Flavell DM, Fruchart JC, Staels B. Characterization of the human PPARalpha promoter: identification of a functional nuclear receptor response element. Mol Endocrinol 2002;16:1013–1028
32. Liu GH, Qu J, Shen X. Thioredoxin-mediated negative autoregulation of peroxisome proliferator-activated receptor alpha transcriptional activity. Mol Biol Cell 2006;17:1822–1833
33. Fisher FM, Kleiner S, Douris N, et al. FGF21 regulates PGC-1α and browning of white adipose tissues in adaptive thermogenesis. Genes Dev 2012;26:271–281
34. Owen BM, Ding X, Morgan DA, et al. FGF21 acts centrally to induce sympathetic nerve activity, energy expenditure, and weight loss. Cell Metab 2014;20:670–677
35. Carr RM, Patel RT, Rao V, et al. Reduction of TIP47 improves hepatic steatosis and glucose homeostasis in mice. Am J Physiol Regul Integr Comp Physiol 2012;302:R996–R1003
36. Kleinert M, Parker BL, Chaudhuri R, et al. mTORC2 and AMPK differentially regulate muscle triglyceride content via Perilipin 3. Mol Metab 2016;5:646–655
37. McManaman JL, Bales ES, Orlicky DJ, et al. Perilipin-2-null mice are protected against diet-induced obesity, adipose inflammation, and fatty liver disease. J Lipid Res 2013;54:1346–1359
38. Cypess AM, Weiner LS, Roberts-Toler C, et al. Activation of human brown adipose tissue by a β3-adrenergic receptor agonist. Cell Metab 2015;21:33–38
39. Mottillo EP, Balasubramanian P, Lee YH, Weng C, Kershaw EE, Granneman JG. Coupling of lipolysis and de novo lipogenesis in brown, beige, and white adipose tissues during chronic β3-adrenergic receptor activation. J Lipid Res 2014;55:2276–2286
40. Haemmerle G, Lass A, Zimmermann R, et al. Defective lipolysis and altered energy metabolism in mice lacking adipose triglyceride lipase. Science 2006;312:734–737
41. Lee J, Ellis JM, Wolfgang MJ. Adipose fatty acid oxidation is required for thermogenesis and potentiates oxidative stress-induced inflammation. Cell Reports 2015;10:266–279
42. Schupp M, Lazar MA. Endogenous ligands for nuclear receptors: digging deeper. J Biol Chem 2010;285:40409–40415
43. Nolte RT, Wisely GB, Westin S, et al. Ligand binding and co-activator assembly of the peroxisome proliferator-activated receptor-gamma. Nature 1998;395:137–143
44. Hondares E, Rosell M, Díaz-Delfín J, et al. Peroxisome proliferator-activated receptor α (PPARα) induces PPARγ coactivator 1α (PGC-1α) gene expression and contributes to thermogenic activation of brown fat: involvement of PRDM16. J Biol Chem 2011;286:43112–43122
45. Mottillo EP, Bloch AE, Leff T, Granneman JG. Lipolytic products activate peroxisome proliferator-activated receptor (PPAR) α and δ in brown adipocytes to match fatty acid oxidation with supply. J Biol Chem 2012;287:25038–25048
46. Fedorenko A, Lishko PV, Kirichok Y. Mechanism of fatty-acid-dependent UCP1 uncoupling in brown fat mitochondria. Cell 2012;151:400–413
47. Varga T, Czimmerer Z, Nagy L. PPARs are a unique set of fatty acid regulated transcription factors controlling both lipid metabolism and inflammation. Biochim Biophys Acta 2011;1812:1007–1022
48. Ohno H, Shinoda K, Spiegelman BM, Kajimura S. PPARγ agonists induce a white-to-brown fat conversion through stabilization of PRDM16 protein. Cell Metab 2012;15:395–404
49. Barbera MJ, Schluter A, Pedraza N, Iglesias R, Villarroya F, Giralt M. Peroxisome proliferator-activated receptor alpha activates transcription of the brown fat uncoupling protein-1 gene. A link between regulation of the thermogenic and lipid oxidation pathways in the brown fat cell. J Biol Chem 2001;276:1486–1493
50. Petrovic N, Walden TB, Shabalina IG, Timmons JA, Cannon B, Nedergaard J. Chronic peroxisome proliferator-activated receptor gamma (PPARgamma) activation of epididymally derived white adipocyte cultures reveals a population of thermogenically competent, UCP1-containing adipocytes molecularly distinct from classic brown adipocytes. J Biol Chem 2010;285:7153–7164
51. Tontonoz P, Hu E, Graves RA, Budavari AI, Spiegelman BM. mPPAR gamma 2: tissue-specific regulator of an adipocyte enhancer. Genes Dev 1994;8:1224–1234
52. Shu L, Hoo RL, Wu X, et al. A-FABP mediates adaptive thermogenesis by promoting intracellular activation of thyroid hormones in brown adipocytes. Nat Commun 2017;8:14147
53. Li P, Zhu Z, Lu Y, Granneman JG. Metabolic and cellular plasticity in white adipose tissue II: role of peroxisome proliferator-activated receptor-alpha. Am J Physiol Endocrinol Metab 2005;289:E617–E626